Thermal resistance of steels with increased strength properties for pressure vessels of advanced VVER reactors of various designs[*]

Evgenia A. Kuleshova[1,2], Ivan V. Fedotov[1], Dmitry A. Maltsev[1],
Margarita G. Isaenkova[2], Olga A. Krymskaya[2], Roman A. Minushkin[2]

1 *National Research Centre "Kurchatov Institute", 1 Akad. Kurchatova Sq., 123182 Moscow, Russia*
2 *National Research Nuclear University "MEPhI", 31 Kashirskoye Sh., 115409 Moscow, Russia*

Corresponding author: Ivan V. Fedotov (ivanxfedotov@yandex.ru)

Abstract

The paper considers the results of structural studies and mechanical tests after a long-term thermal exposure of laboratory heats of the metallurgically improved 15Kh2NMFA steel and steel with an increased content of nickel considered as materials for the pressure vessels of advanced VVER-type reactors of various designs. It has been shown that, both for the improved 15Kh2NMFA steel and the high-nickel steel, there are no signs of grain boundary embrittlement after an segregation provoking embrittlement heat treatment. This is explained by the extremely low grain boundary segregation of phosphorus in the initial state caused by a high degree of the structure dispersity as well as by rather a low content of impurities. Besides, no changes have been found in the yield strength value for the improved 15Kh2NMFA steel, which agrees with the structure investigation results. For the high-nickel steel, a tendency towards a minor yield strength decrease by 5 to 10% and a regular reduction of the critical brittleness temperature has been revealed. A decrease in the mechanical properties has been caused by a relatively low temperature of tempering for the high-nickel steel and, accordingly, by the potential occurrence of the structure recovery during long-term thermal exposure, as evidenced by the results of an X-ray diffraction analysis. Despite the structure recovery in the high-nickel steel under the long-term thermal exposure, the main strengthening carbide phases remain stable. Due to this, the yield strength value remains at a relatively high level that exceeds the values for the modern VVER-type vessel steels, even in the case of a thermal exposure much in excess of the expected operating conditions for advanced VVER reactors. The observed decrease of critical brittleness temperature during the long-term thermal exposure contributes to an increase in the steel resistance to brittle fracture.

* Russian text published: Izvestiya vuzov. Yadernaya Energetika (ISSN 0204-3327), 2023, n. 2, pp. 93–106.

Introduction

The evolution of Russian nuclear power suggests increasing the efficiency of the VVER reactors, the most commonly used reactor type, through extending their lifetime, upgrading the reactor core (regulating the neutron spectrum) and improving the coolant parameters (Alekseev 2016). This undoubtedly entails tougher conditions of operation and increased requirements to the reactor pressure vessel (RPV) material which requires, in turn, more high-performance materials (Markov et al. 2016).

Increasing the nickel content in low-carbon steels is efficient in terms of improving both the strength and toughness characteristics which creates opportunities for improving the mechanical performance of steels used in current reactor pressure vessels (Markov et al. 2016; Pratomo et al. 2019). However, the accumulated experience in exploring the VVER RPV steels shows that an increase in the content of Ni leads, under certain conditions, to an increased rate of their thermal and irradiation embrittlement (Shtrombakh et al. 2015; Kuleshova et al. 2021). In particular, Ni intensifies the grain boundary segregation of phosphorus which causes a decrease in the cohesive strength of the grain boundaries and leads to an increase of critical temperature of brittleness (T_K) due to a decrease in brittle intergranular fracture stress (Shtrombakh et al. 2015). Limited content of some alloying elements and high purity are known to contribute to a better thermal and radiation resistance of high-nickel steels (Balandin et al. 1984; Lee et al. 2010). In connection with this, under development are high-strength RPV steels for advanced VVERs based on the 15Kh2NMFA steel (strength grade (KP) 50–55) and high-nickel steels with the nickel content of up to 4 to 5 wt. % (KP 65+ grade) (Markov et al. 2016). To confirm the possibility for using these steels as the RPV materials for advanced VVERs, it is required to confirm their thermal resistance, specifically resistance to grain boundary embrittlement in the expected operation conditions.

Earlier, in Kuleshova et al. 2022a, 2022b, the structural-phase state of high-nickel RPV steels for advanced VVERs was investigated and structural featureы were defined which contribute to improving their strength properties, as well as to the low value of critical temperature of brittleness in the initial state.

This paper presents and analyzes the results of structural studies and mechanical tests after the long-term thermal exposures obtained at NRC Kurchatov Institute for laboratory heats of higher-strength RPV steels with increased Ni content developed at TsNIITMASh JSC.

Materials and methods

Materials

Comparative studies have been conducted for the developed at TsNIITMASh JSC: 15Kh2NMFA steel of class 1 (reference steel), metallurgically improved 15Kh2NMFA steel, and high-nickel steel of different laboratory heats. Specific to these steels is a very low content of impurities, wt. %: P (< 0.005), S (< 0.003) and Cu (0.01–0.003) with the total content of carbide-forming elements (Cr+Mo+V+Nb) in a range of 2.0 to 3.0 wt. %.

Table 1 presents the characteristics of the investigated steels. The heat treatment mode parameters for the high-nickel steel differs in a lower temperature of tempering than for 15Kh2NMFA-type steels.

Table 1. Characteristics of tested materials

Steel	Index	Heat	Strength grade	Ni content, wt. %	Grain size, μm
15Kh2NMFA, class 1	BM-0	-	KP45	1.18	35
15Kh2NMFA, improved	BM-1	-	KP50-55	1.57	8
High-Ni steel	BM-2	No. 1	KP65+	4.07	40
		No. 2		5.26	7–12
		No. 3–No. 6		5.0–5.6	

To estimate the resistance of the investigated steels to grain boundary embrittlement as a result of the reversible temper embrittlement (Balandin et al. 1984), and to estimate the stability of their structural parameters and mechanical characteristics, an embrittlement heat treatment (EHT) mode has been developed. An embrittlement heat treatment is expected to cause the intensive accumulation of grain boundary phosphorus segregation in the investigated steels (Table 2).

A box furnace of the SNOL-2.2,5.1,8/10-I7 type was used for the EHT. The steels were heated at the maximum furnace power up to the first exposure step (600 °C) and cooled to room temperature after the last exposure step (460 °C) at a rate ~20 °C/h.

Table 2. The mode of developed embrittlement heat treatment

Temperature of step, °C	600	590	580	570	560	550	540	530
Exposure time, h	3	4	6	9	13	19	28	43
Temperature of step, °C	520	510	500	490	480	470	460	-
Exposure time, h	67	104	164	261	422	690	1144	-

To estimate the stability of the phase structural state and characteristics of the high-nickel steel, high-nickel steel heats were also examined after a long-term isothermal exposure (IE) in a range of 450 to 550 °C for hundreds and thousands of hours.

To generalize the investigation results and identify the trends for changes in the structural parameters and the mechanical characteristics as a result of a long-term thermal exposure, the investigated states parameters were reduced to the Hollomon-Jaffe parameter (Holloman and Jaffe 1945):

$$H_P = [(T + 273) \cdot (20 + \log(t))]/100 \qquad (1)$$

where T is the exposure temperature, °C, and t is the time of the thermal exposure, h.

The EHT mode was also reduced to parameter H_p using expression (1) by way of recounting each step in terms of the equivalent exposure time with an average temperature of 500 °C.

Mechanical tests

To detect the changes in the strength characteristics of steels as a result of a long-term thermal exposure, uniaxial static tension tests and microhardness measurements were conducted. The static tension tests were conducted on cylindrical specimens with the test part diameter of 3.0 mm. The tension test results were processed and the yield strength ($\sigma_{0.2}$) was determined in accordance with GOST 1497-84. Microhardness was measured using metallographic specimens in accordance with GOST R ISO 6507-1-2007.

To identify the embrittlement effects as a result of a EHT, impact bending tests were conducted with determining critical temperature of brittleness T_K, that characterizes the ductile-brittle transition temperature for RPV steels. The impact bending tests were conducted on Charpy-type test specimens. The impact bending test results were processed and T_K was determined as defined in Appendix E to GOST R 50.05.12-2018.

Investigation by transmission and scanning electron microscopy

The qualitative analysis of sizes and number densities for the main strengthening carbide phases in the investigated steels was undertaken by transmission electron microscopy (TEM) using a Titan 80–300 high-resolution microscope (FEI, the USA), as well as using scanning electron microscopy (SEM) using a Merlin high-resolution field emission scanning electron microscope (Zeiss, Germany).

Specimens for TEM and SEM investigations were prepared by method of two-side electrochemical polishing. Thinning was done with the use of Struers Tenupol 5 device within 10% $HClO_4$ solution in methanol at the temperature below minus 50 °C and voltage about 20 V.

Fractographic investigation

Fractographic investigation of the tested specimen fracture surface makes it possible to obtain direct information about the failure mechanisms, specifically the degree of the grain boundary embrittlement in steel, based on the change in the portion of brittle intergranular fracture (correlates with the grain boundary segregation level) (Naudin et al. 1999; Kameda and Nishiyama 2011; Shtrombakh et al. 2014). For example, for typical RPV steels the portion of brittle intergranular fracture of ≤ 5% shows that the level of the phosphorus grain boundary segregation (C_p) does not exceed 10 to 15% of the phosphorus monolayer coverage and does not have a regular effect on the shift in the critical temperature of brittleness (Naudin et al. 1999; Kameda and Nishiyama 2011; Fedotova et al. 2019).

The fractographic investigation of the Charpy specimens fracture surface after the impact bending tests was carried out using a Supra 40-VP field emission raster electron microscope (Zeiss, Germany). The secondary electron images were acquired with accelerating voltages of 10 to 20 kV in a magnification interval of ×50 to ×3000. The portion of brittle intergranular fracture was determined using the Glagolev method (Saltykov 1970).

Investigation of grain boundary segregation by the Auger electron spectroscopy method

The chemical composition of the grain boundary segregation was investigated by the Auger electron spectroscopy (AES) method on the fractures of cylindrical specimens with circular notche (diameter 3.2, height 18 mm) using an Auger Nanoprobe 700 scanning electron microscope (PHI-Ulvac, USA and Japan). The specimen fracture was obtained using a high-vacuum microscope device which was cooled together with the specimen in liquid nitrogen at a pressure ≤$7 \cdot 10^{-10}$ torr. The level of the phosphorus grain boundary segregation as the percentage of the monolayer coverage (C_p) was determined on the intergranular fracture facets.

X-ray investigation

To determine the phase composition of specimens and evaluate their structural state, diffraction spectra were recorded using a D8 DISCOVER with DAVINCI diffractometer (Bruker, Germany) at the MEPhI's Laboratory of X-Ray Texture Analysis. Co K_α radiation was used as it has less absorption coefficient in steel in comparison with widely used Cu K_α. BrukerAXS DIFFRAC.EVA v.4.2 software and international database ICDD PDF-2 were used for phase identification. Processing of experimental specter data was done by usage of Rietveld method in the software DIFFRACT. TOPAS v.5.0. The average size of the coherent scattering regions (D) and microdeformation (ε_{micro}) was estimated based on analyzing the intrinsic broadening of X-ray lines using expressions (Ungar 2004; Ungar et al. 2005):

$$\beta \cos\theta = (\lambda/D) + 4<\varepsilon_{micro}>\sin\theta, \qquad (2)$$

where β is the integral width of the diffraction maximum, λ is wavelength of the radiation used, D is the average size of the coherent scattering regions, θ is the Bragg angle of the recorded reflection, and ε_{micro} is microdeformation.

Experimental results and discussion

Static tension tests and microhardness measurements

Fig. 1 presents values of yield strength, $\sigma_{0.2}$, and microhardness, $HV_{0.1}$, for the tested steels in the initial state and after a long-term thermal exposure with different parameters, as well as their comparison with the test results for the reference 15Kh2NMFA class 1 steel.
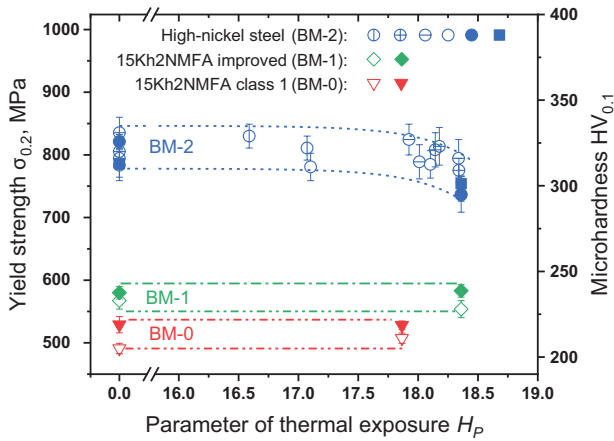
Figure 1. Yield strength, $\sigma_{0.2}$, (solid symbols) and microhardness, $HV_{0.1}$, (open symbols) compared for the tested steels in the initial state and after a long-term thermal exposure with different parameters.

It can be seen from the data presented in Fig. 1 that both for the improved 15Kh2NMFA steel and the reference 15Kh2NMFA class 1 steel there is a typical (Shtrombakh et al. 2015) for the RPV steels constancy of the $\sigma_{0.2}$ and $HV_{0.1}$ values even after thermal exposures with relatively high values of the parameter $H_P = 17.8$–18.3.

It can be also seen that there is a trend for high-nickel steels towards a minor decrease in the $\sigma_{0.2}$ and $HV_{0.1}$ values (by 5 to 10%) for different heats after relatively high values of the thermal exposure parameter ($H_P > 18.2$). For some high-nickel steel heats, no $HV_{0.1}$ reduction has been however observed. Still, on the whole, the $\sigma_{0.2}$ values for the high-nickel steel remain at rather a high level (> 700 MPa), exceeding greatly the typical values for the 15Kh2MFA- and 15Kh2NMFA-type steels currently used as the VVER RPV materials.

Impact bending tests

The impact bending tests were conducted for different high-nickel steel heats after a segregation provoking embrittling heat treatment (EHT), since after EHT the greatest increase of the T_K shift are expected due to passage through the entire temperature interval with the maximal effects of the reversible temper brittleness. Table 3 presents the T_K values for the tested steels in the initial state and after the EHT.

It can be seen from the table that there is a typical for the RPV steels (Shtrombakh et al. 2015) shift in T_K for the 15Kh2NMFA class 1 steel after the EHT caused by the accumulation of the grain boundary segregation of phosphorus. For the improved 15Kh2NMFA steel with a higher content of Ni, as compared with the 15Kh2NMFA class 1 steel, the post-EHT T_K value is at the initial state level. This indicates to a higher resistance of the improved 15Kh2NMFA steel against temper embrittlement, despite its increased content of Ni that usually intensify the phosphorus segregation processes and the grain boundary embrittlement respectively (Shtrombakh et al. 2015). It can be also seen that there is untypical for the RPV steels T_K change towards lower temperatures after EHT. To clarify the reasons for the identified features of changes in the mechanical characteristics of the studied steels after EHT, a complex of structural studies was carried out.

Fractographic and AES investigation of the grain boundaries

Table 3 presents the fractographic and AES investigation results for different steels after the EHT. For the high-nickel steel, however, no results have been provided by the AES investigation due to the absence of brittle intergranular fracture regions in the AES specimens, which indicates, in turn, to a high cohesive strength of the grain boundaries.

For the improved 15Kh2NMFA steel with a higher content of Ni, as compared with the 15Kh2NMFA class 1 steel, just a slight difference has been found in the portion of brittle intergranular fracture, v, in the initial state which agrees with the absence of a T_K change. The absence of T_K changes and a small portion of brittle intergranular fracture, v, for the investigated steel was caused by a very low level of the grain boundary phosphorus segregation, C_P, not only in the initial state but also after the EHT which is not enough for the T_K shift into higher temperatures region (Naudin et al. 1999; Kameda and Nishiyama 2011; Fedotova et al. 2019). The low value of C_P in the improved 15Kh2NMFA steel in the initial state can be explained by a four times smaller grain size and, accordingly, by extended length of grain boundaries which is expected to the distribution of the existing phosphorus through a large surface area.

For the high-nickel steel, no change in the portion of brittle intergranular fracture in the Charpy specimens was found after the EHT which agrees with the absence of a T_K

Table 3. Fractographic and AES in vestigation and impact bending test results for investigated steels after EHT

Steel	Average grain size, μm	Critical brittleness temperature T_K, °C		Maximum portion of brittle intergranular fracture v, %		Grain boundary segregation of phosphorus C_P, % of P monolayer coverage	
		Initial state	Post-EHT	Initial state	Post-EHT	Initial state	Post-EHT
15Kh2NMFA, class 1	35	-90	-55	<5	30	8–10	22–24
15Kh2NMFA, improved	8	-74	-75	0	<5	2–3	<10–15
High-nickel steel	40	-90	-133	0	0	ND	ND
	10	-131	-140	0	0	ND	ND

ND – not determined due to the absence of brittle intergranular fracture.

shift into the higher temperature region (see Table 3). The earlier detected (Kuleshova et al. 2022b) increase in the structural dispersion degree for the high-nickel steels with extended length of high-angle boundaries, as well as the improved purity of steel in terms of the impurity content also defines the low level of the grain boundary phosphorus segregation, C_P, and, accordingly, the absence of brittle intergranular fracture in the initial state and after the EHT.

Structural investigation of steels

Fig. 2 presents the characteristics (average size d and number density N) of small (MeC or Me_2C type (Kuleshova et al. 2022b) and large (Me_3C, Me_7C_3, Me_2C, NbC and other type (Kuleshova et al. 2022b) precipitate of the main strengthening carbide phases for the improved 15Kh2NMFA steel, as well as for the high-nickel steel heats with the largest effects of the $HV_{0.1}$ and $\sigma_{0.2}$ reduction in various states. Table 4 presents the differences in the contributions of precipitation hardening ($\Delta\sigma_d$), estimated taking into account the Orowan-Ashby equation (Kuleshova et al. 2022b), between the initial state and the state after a long-term thermal exposure for the tested steels.
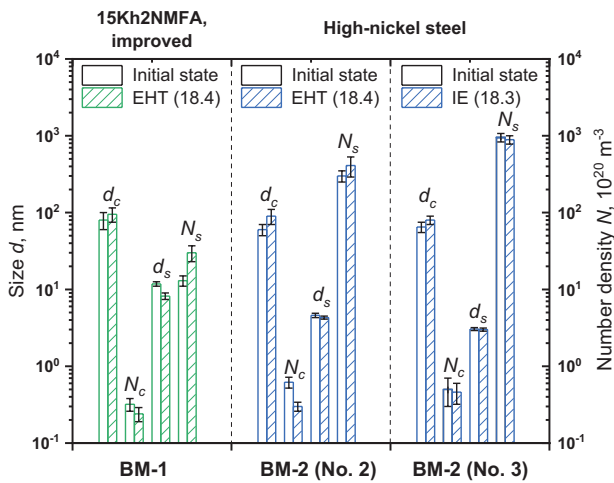

Figure 2. Average size, d, and number density, N, of small nanosized (d_s, N_s) and coarse (d_c, N_c) precipitates of the carbide phases in tested steels in various states (EHT – embrittling heat treatment, IE – isothermal exposure; shown in brackets is the value of parameter H_P corresponding to thermal exposure).

It can be seen from the data in Fig. 2 and in Table 4 that both for 15Kh2NMFA-type steels and different high-nickel steel heats, there are no differences in the characteristics of the carbide phase precipitates (size and number density) in terms of precipitation hardening after a long-term thermal exposures (EHT and IE). Specifically, this is evidenced by the absence of a correlation between the differences in the contribution of precipitation hardening and by the change in the yield strength for the tested steels (see Table 4).

It should be noted that, along with carbide phases, the high-nickel steel structure includes a small fraction (1 to 2%) of residual austenite (Kuleshova et al. 2022b),

Table 4. Estimated differences in the contributions of precipitation hardening between the initial state and the state after a long-term thermal exposure for tested steels

Steel	Heat	Thermal exposure		Change in yield strength $\Delta\sigma_{0.2}$, MPa	Change in precipitation hardening $\Delta\sigma_d$, MPa
		Type	Parameter H_P		
15Kh2NMFA, class 1	-	EHT	17.8	-1*	+18
15Kh2NMFA, improved	-	EHT	18.4	+3	+5
High-nickel steel	No. 2	EHT	18.4	-80	+30
	No. 3	IE	18.3	-60**	-10

* – based on data Shtrombakh et al. 2015; ** – recounted from $HV_{0.1}$.

transformation (dissolution) of which can affect, accordingly, the characteristics of the structure and the mechanical performance of steel (Akhavan et al. 2011). It has been found as a result of the X-ray phase investigation that the volume fraction of residual austenite in a high-nickel steel remains at the initial level (1 to 2%) after a long-term thermal exposure, which is the evidence of its stability in the thermal exposure conditions under consideration.

Table 5. Generalized characteristics of the tested steel structures in the initial state and after a long-term thermal exposure

Material	Size of coherent scattering regions D, nm		Microdeformation $<\varepsilon_{micro}>$, %	
	Initial state	After long-term thermal exposure	Initial state	After long-term thermal exposure
15Kh2NMFA, improved	196 ± 60	210 ± 20	0.03 ± 0.01	0.02 ± 0.01
High-nickel steel	90 ± 15	150 ± 30	0.05 ± 0.01	0.04 ± 0.02

For the tested steels, Table 5 generalizes the integral characteristics of the structure (average size of coherent scattering regions, D, and microdeformation values, $<\varepsilon_{micro}>$), obtained as the result of analyzing the X-ray line broadening in the initial state and after a long-term thermal exposure.

It can be seen from the data presented in Table 5 that, for the high-nickel steel, a long-term thermal exposure results in an increase observed in the size of the coherent scattering regions and a decrease in the microdeformations, which is not typical so much for the improved 15Kh2NMFA steel. The key factors that affect the physical broadening of X-ray lines, which evidences the change in the size of the coherent scattering regions and value of microdeformations, are density of the substructural boundaries and characteristics of the dislocation structure (Ungar 2004; Ungar et al. 2005). A high-temperature tempering process is known to involve processes of the equilibrium substructure formation in steel, which are accompanied by the dislocation structure and structural boundary rearrangement (Markov 2012). For example, these processes for the 15Kh2NMFA steel are over at high-temperature tempering for 50 hours under 650 °C (Markov 2012), which corresponds to a thermal exposure of

$H_P \approx 20$ (see equation (1)). The high-temperature tempering conditions for the improved 15Kh2NMFA steel correspond to $H_P \approx 21$, and parameter H_P for the high-nickel steel is smaller and is close to $H_P \approx 19$ due to a lower tempering temperature. A smaller value of parameter H_P at the high-nickel steel high-temperature tempering stage indicates to a smaller intensity of the thermal effect, which could lead to the incomplete equilibrium substructure formation in the initial state and the respective yield strength reduction in the event of a further long-term thermal exposure.

At the same time, the observed reduction of T_K for the high-nickel steel in accordance with the Ioffe scheme (El-manov et al. 2021) can be explained by the revealed trend for a decrease in the yield strength of the high-nickel steel as a result of a long-term thermal exposure (see Fig. 1). However, no direct proportionality between the yield strength change and the shift in T_K has been found in the study. Thus, for example, the greatest shift in T_K is not matched by the greatest change in the yield strength. Therefore, a reduction of both $\sigma_{0.2}$ and T_K for different heats of high-nickel steel may indicate that the effects in question are expectable, and the absence of proportionality between the changes in $\sigma_{0.2}$ and T_K is the evidence of a major role played in these effects by the scatter in properties for the material.

It should be noted that despite the trend identified for high-nickel steel towards a minor decrease in the yield strength (by 5 to 10%) and the respective decrease in T_K in the course of a long-term thermal exposure, high-nickel steel is characterized by much higher yield strength values as compared with traditional VVER RPV steels (see Fig. 1). The yield strength of high-nickel steel is most likely to be preserved at rather a high level (KP65+) after a long-term thermal exposure, which is achieved through the stability of the main strengthening carbide phases (see Fig. 2). And the provided estimations are relatively conservative since the expected conditions of service for the tested steels are matched by a much smaller thermal exposure ($H_P < 18$) and, accordingly, by a smaller decrease of $\sigma_{0.2}$ in the course of service. Besides, the identified decrease in the T_K value for high-nickel steel as a result of a long-term thermal exposure just contributes to the increased brittle fracture resistance of steel in the process of service as part of the RPV thanks to the potential compensation of the irradiation embrittlement that leads to the increase of T_K typical of traditional RPV steels of the 15Kh2MFA and 15Kh2NMFA types. Therefore, the identified peculiarities of the improved 15Kh2NMFA and high-nickel steel behavior during a long-term thermal exposure create opportunities for these steel to be used as the RPV materials in advanced VVER reactors of different designs.

However, in the process of the reactor operation, apart from thermal effects, the RPV material is also subjected to combined effects of neutron irradiation and mechanical loads, which may cause the steel structure and properties to degrade. In this connection, confirming the possibility of using the improved 15Kh2NMFA steel and high-nickel steel as the advanced VVER RPV material requires undertaking complex structural studies and mechanical tests, including for commercial metals, which will be done in future.

Conclusions

It was identified as a result of mechanical tests and structural studies for the laboratory heats of the improved 15Kh2NMFA steel and high-nickel steel after a long-term thermal exposure that:

1. There are no signs of grain boundary embrittlement as a result of provoking embrittling heat treatment for the improved 15Kh2NMFA steel and high-nickel steel. This is evidenced by the absence of brittle intergranular fracture, as well as the absence of the T_K shift into a higher temperature region and indicates to a high resistance of steels to temper embrittlement thanks to a very low level of grain boundary segregation.
2. Low level of the grain boundary segregation of phosphorus in the improved 15Kh2NMFA steel and high-nickel steel is caused, along with high purity of the steel in terms of impurity contents, by the extended length of structural boundaries due to small grains and a more dispersed structure.
3. Specific to high-nickel steel with relatively high values of the thermal exposure parameters ($H_P > 18.2$) is a 5 to 10% yield strength and microhardness decrease, which is accompanied by the expectably achieved lower values of T_K, as compared with the initial state, and is likely to be attributed to the steel structure recovery processes during a long-term thermal exposure.
4. Despite a certain decrease in the mechanical properties of high-nickel steel during a long-term thermal exposure, they remain at a sufficiently high level thanks to the stability of the main strengthening carbide phases.

A further stage in the activities to investigate the advanced VVER RPV steels under development is to verify the mechanical propertied with confirming respectively their sufficient thermal and radiation resistance, including based on commercial metals.

References

■ Akhavan Tabatabae B, Ashrafizadeh F, Hassanli AM (2011) Influence of retained austenite on the mechanical properties of low carbon martensitic stainless steel castings. ISIJ International 51(3): 471–475. https://doi.org/10.2355/isijinternational.51.471

■ Alekseev PN (2016) Directions for the development of the nuclear power system. Innovatika i Ekspertiza 3(18): 67–80. https://elibrary.ru/download/elibrary_29032662_68651559.pdf [accessed Feb. 01, 2023] [in Russian]

- Balandin YuF, Gorynin IV, Zvezdin YuI, Markov VG (1984) NPP Structural Materials. Enegoatomizdat Publ., Moscow, 280 pp. [in Russian]

- Elmanov GN, Zaluzhny AG, Skrytny VI, Smirnov EA, Perlovich YuA, Yalcev VN (2021) Volume 1. Solid State Physics. Physical Materials Science: Textbook for Universities: in 8 v., ed. by B.A. Kalin, ed. 3, MEPhI Publ., Moscow, 764 pp. [ISBN 978-5-7262-2725-2] [in Russian]

- Fedotova SV, Kuleshova EA, Maltsev DA, Saltykov MA (2019) Complex study of grain boundary segregation in long-term irradiated reactor pressure vessel steels. Journal of Nuclear Materials 528(151865): 1–8. https://doi.org/10.1016/j.jnucmat.2019.151865

- Holloman JH, Jaffe JH (1945) Time-temperatures relations in tempering steel. Transactions of the American Institute of Mining and Metallurgical Engineers 162: 223–249.

- Kameda J, Nishiyama Y (2011) Combined effects of phosphorus segregation and partial intergranular fracture on the ductile-brittle transition temperature in structural alloy steels. Materials Science and Engineering A 528(10–11): 3705–713. https://doi.org/10.1016/j.msea.2011.01.018

- Kuleshova EA, Zhuchkov GM, Fedotova SV, Maltsev DA, Frolov AS, Fedotov IV (2021) Precipitation kinetics of radiation-induced Ni-Mn-Si phases in VVER-1000 reactor pressure vessel steels under low and high flux irradiation. Journal of Nuclear Materials 553(153091): 1–11. https://doi.org/10.1016/j.jnucmat.2021.153091

- Kuleshova EA, Fedotov IV, Maltsev DA, Frolov AS, Stepanov NV, Safonov DV (2022a) The role of nickel in the formation of a structure that provides improved service characteristics of reactor structural materials. Izvestiya vuzov. Yadernaya Energetika 3: 120–133. https://doi.org/10.26583/npe.2022.3.11 [in Russian]

- Kuleshova EA, Fedotov IV, Maltsev DA, Potekhin AA, Bubyakin SA, Isaenkova MG, Krymskaya OA, Minushkin RA (2022b) Structural features ensuring the increase of service characteristics of high-nickel steels for pressure vessels of prospective energy-generation reactors. International Journal of Pressure Vessels and Piping 200(104845): 1–13. https://doi.org/10.1016/j.ijpvp.2022.104845

- Lee BS, Kim MC, Yoon JH, Hong JH (2010) Characterization of high strength and high toughness Ni-Mo-Cr low alloy steels for nuclear application. International Journal of Pressure Vessels and Piping 87(1): 74–80. https://doi.org/10.1016/j.ijpvp.2009.11.001

- Markov SI (2012) Metallurgical Foundations for the Production of Blanks for Highly Reliable Elements of Energy and Pipeline Systems. Dr. Sci. (Engineering) Diss. OAO NPO "CNIITMASH" Publ., Moscow, 83 pp. [in Russian]

- Markov SI, Dub VS, Lebedev AG, Kuleshova EA, Balikoev AG, Makarycheva EV, Tolstykh DS, Frolov AS, Krikun EV (2016) Advanced reactor vessel steels for reactors with supercritical coolant parameters. Russian Metallurgy (Metally) 9: 803–811. https://doi.org/10.1134/S003602951609010X

- Naudin C, Frund JM, Pineau A (1999) Intergranular fracture stress and phosphorus grain boundary segregation of a Mn-Ni-Mo steel. Scripta Materialia 40(9): 1013–1019. https://doi.org/10.1016/S1359-6462(99)00069-X

- Pratomo SB, Oktadinata H, Widodo TW (2019) Effect of Nickel Additions on microstructure evolution and mechanical properties of low-alloy Cr-Mo cast steel. IOP Conference Series: Materials Science and Engineering 541(012050): 1–8. https://doi.org/10.1088/1757-899X/541/1/012050

- Saltykov SA (1970) Stereometric Metallography. Ed. 3, rev. Metallurgiya Publ., Moscow, 376 pp. [in Russian]

- Shtrombakh YI, Gurovich BA, Kuleshova EA, Frolov AS, Fedotova SV, Zhurko DA, Krikun EV (2015) Effect of Ni content on thermal and radiation resistance of VVER RPV steel. Journal of Nuclear Materials 461: 292–300. https://doi.org/10.1016/j.jnucmat.2015.02.023

- Shtrombakh YI, Gurovich BA, Kuleshova EA, Maltsev DA, Fedotova SV, Chernobaeva AA (2014) Thermal ageing mechanisms of VVER-1000 reactor pressure vessel steels. Journal of Nuclear Materials 452(1–3): 348–358. https://doi.org/10.1016/j.jnucmat.2014.05.059

- Ungar T, Tichy G, Gubicza J, Hellmig RJ (2005) Correlation between subgrains and coherently scattering domains. Powder Diffraction PDJ 20(4): 366–375. https://doi.org/10.1154/1.2135313

- Ungar T (2004) Microstructural parameters from X-ray diffraction peak broadening. Scripta Materialia 51(8): 777–781. https://doi.org/10.1016/j.scriptamat.2004.05.007